

SIMULATION OF ELECTRON-CLOUD HEAT LOAD FOR THE COLD ARCS OF THE LARGE HADRON COLLIDER

H. Maury Cuna^{*}, G. Iadarola[†], G. Rumolo, F. Zimmermann, CERN, Geneva, Switzerland

Abstract

The heat load due to the electron cloud in the Large Hadron Collider (LHC) cold arcs is a concern for its performance near and beyond nominal beam current. We report the results of simulation studies, which examine the electron-cloud induced heat load for different values of low-energy electron reflectivity and secondary emission yield at injection energy, as well as at beam energies of 4 TeV and 7 TeV, for two different bunch spacing: 25 ns and 50 ns. Benchmarking the simulations against heat-load observations at different beam energies and bunch spacings allows an estimate of the secondary emission yield in the cold arcs of the LHC and of its evolution as a function of time.

INTRODUCTION

A primary concern for the LHC is the additional heat load due to the electron cloud that is deposited on the beam screen, a perforated tube inserted into the cold bore of the superconducting magnets in order to protect the cold bore from synchrotron radiation and ion bombardment [1]. Electrons released into the vacuum chamber, amplified via secondary emission from the chamber wall through a beam-induced multipacting process, give rise to an electron cloud. The incident cloud electrons heat the beam screen, for which only a limited cooling capacity is available. If the beam-screen heat load exceeds the available cooling the cold superconducting magnets of the LHC arcs, surrounding the beam pipe, will quench; i.e., they lose their superconducting state. Thereby, the electron cloud may limit the maximum permissible beam current of the LHC. The expected heat load does not only depend on the beam current, but also on the bunch spacing, bunch intensity and the time-dependent surface properties of the beam screen. The principal sources of primary electrons are the ionization of the residual gas at injection energy and photoemission at higher energies.

SURFACE PARAMETERS

The secondary emission yield is a time-dependent surface parameter that describes the average number of secondary electrons emitted per incident electron. It is a function of the energy of the primary incident electron and of its angle of incidence. Another important surface parameter is the low-energy electron reflectivity R that designates the probability for an elastic reflection of an electron hitting the wall in the limit of zero primary energy ($0 < R < 1$).

PHOTOEMISSION MODEL

Photoemission from synchrotron radiation provides a copious source of primary electrons. The assumed creation rate of primary photoelectrons, of order $0.6\text{--}1.2 \times 10^{-3}$ per proton and per meter, corresponds to the computed synchrotron radiation flux in the arcs and the photoelectron generation rate, $n_e'[(e/p)/m]$, inferred from measurements with test beams on prototype chambers before or after surface scrubbing. Closely related, the measured photoelectron yield per absorbed photon and per meter, Y^* , is about 5.0% and 2.5% at a maximum secondary-emission yield δ_{max} of 1.9 and 1.1, respectively [2, 3]. During scrubbing, the parameter ε_{max} (the energy corresponding to the maximum secondary emission yield δ_{max}) also changes, from about 249 to 230 eV [4-6]. We linearly interpolate $n_e'[(e/p)/m]$ and ε_{max} as a function of δ_{max} , from the quoted pairs of values, as is illustrated in Table I, which shows a list of surface parameter combinations assumed in our simulations. The number of photons is proportional to beam energy, and the photon energy is proportional to the third power of beam energy. From these scaling laws we expect the number of photoelectrons at 4 TeV to be lower than at 7 TeV by a factor between $4/7$ and $(4/7)^4$. Therefore, for the case of 4 TeV we reduced the photoelectron yield (reported in Table 1) by an intermediate factor of $3/20$. The low energy electron reflectivity was varied between 0.3 and 0.7.

Table 1: Surface parameters used in the simulations sets. The parameter n_e' denotes the rate of primary photoelectrons emitted per proton per meter at 7 TeV beam energy, and Y^* is the associated photoemission yield per absorbed photon.

δ_{max}	ε_{max} (eV)	$n_e'[(e/p)/m]$	$Y^* [e/(abs)\gamma]$
1.1	230.0	5.80×10^{-4}	0.025
1.2	232.4	6.53×10^{-4}	0.028
1.3	234.7	7.25×10^{-4}	0.031
1.4	237.1	7.98×10^{-4}	0.034
1.5	239.5	8.71×10^{-4}	0.037
1.6	241.9	9.43×10^{-4}	0.041
1.7	244.2	1.02×10^{-3}	0.044

SIMULATION METHODOLOGY

We performed two sets of simulations in order to determine the heat load values at 50 ns at injection energy

^{*}Also at CINVESTAV-IPN, Merida Campus, Merida, Mexico

[†]Also at Università degli Studi di Napoli Federico II, Napoli, Italy

and 4 TeV, with actual emittances (at this bunch spacing) which are smaller than the design value. A third set of simulations was conducted in order to obtain an updated prediction for 7 TeV beam energy and the nominal 25-ns bunch spacing. For the case of 50-ns bunch spacing we considered the actual filling pattern used in operation, with 1380 bunches per beam. The details of this filling pattern are described in Ref. [7]. For the case of 25 ns, we took the nominal LHC filling pattern with 2808 bunches per beam [8]. The surface and simulation parameters assumed are listed in Tables 1 and 2. All the simulations were performed for a bending section using the newly developed electron-cloud simulation code: PyECLoud [9]. We assumed a Gaussian bunch profile.

Table 2: Summary of simulation parameters.

Parameter	450 GeV	4 TeV	7 TeV
Bunch intensity	1.15×10^{11} p/b	1.15×10^{11} p/b	1.15×10^{11} p/b
RMS bunch length	11.8 cm	9 cm	7.55 cm
Bunch spacing	50 ns	50 ns	25 ns
Transverse normalized emittance	2 μm rad	2.5 μm rad	3.75 μm rad
Pressure	32 nTorr	---	---

RESULTS

In Fig. 1 the simulated heat load values for a dipole magnet at 7 TeV and 25-ns bunch spacing are presented. As we can see, in order to achieve a heat load smaller than the maximum cooling capacity of about 1 W/m it is necessary to reduce the secondary emission yield to values below 1.4, if we want to operate the LHC with the nominal parameters at this energy range. This result is quite insensitive to the value of the low-energy reflectivity R .

Figure 2 shows the simulated heat load values for a dipole section at 4 TeV and 50-ns bunch spacing. This bunch spacing gives much smaller heat-load values and according to simulations for this operational scheme the electron cloud is of no concern with regard to the cooling capacity.

In Fig. 3 we report the 50-ns results at injection energy. As we observe these values are smaller than those at 4 TeV for one order of magnitude.

Finally, in Fig. 4 we show the evolution of the secondary emission yield over a period of 1 year (2011).

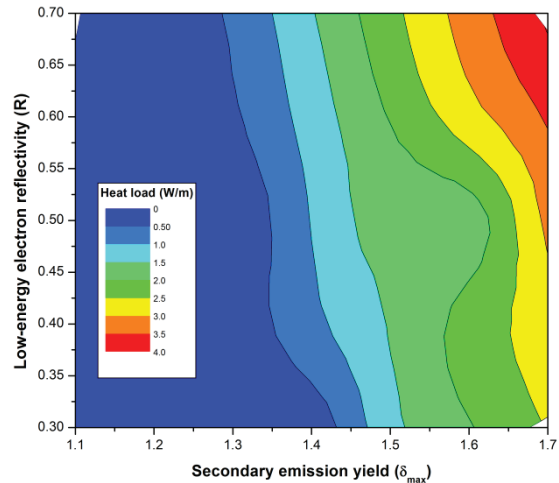


Figure 1: Simulated heat load values for a dipole section at 7 TeV and 25-ns bunch spacing.

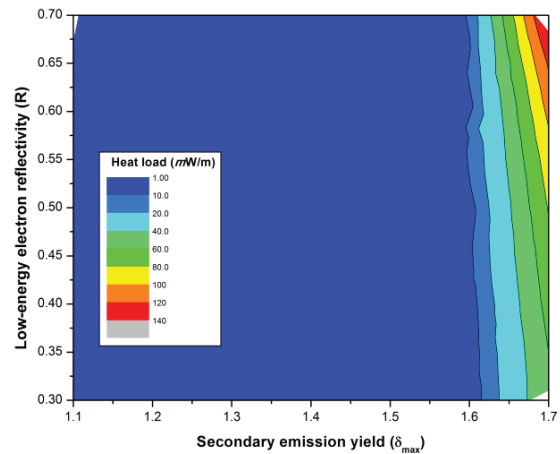


Figure 2: Simulated heat load values for a dipole section at 4 TeV and 50-ns bunch spacing.

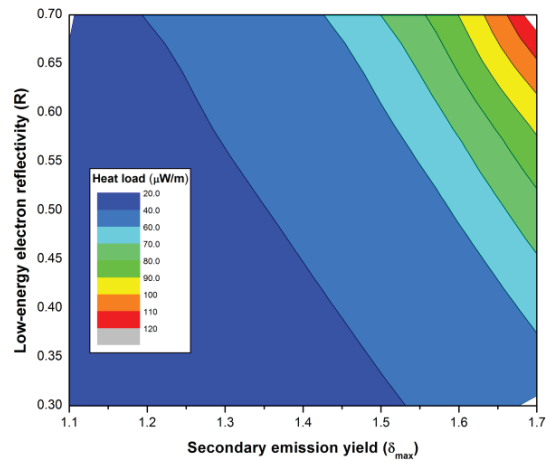


Figure 3: Simulated heat load values for a dipole section at 450 GeV and 50-ns bunch spacing.

Copyright © 2012 by IEEE – cc Creative Commons Attribution 3.0 (CC BY 3.0) — cc Creative Commons Attribution 3.0 (CC BY 3.0)

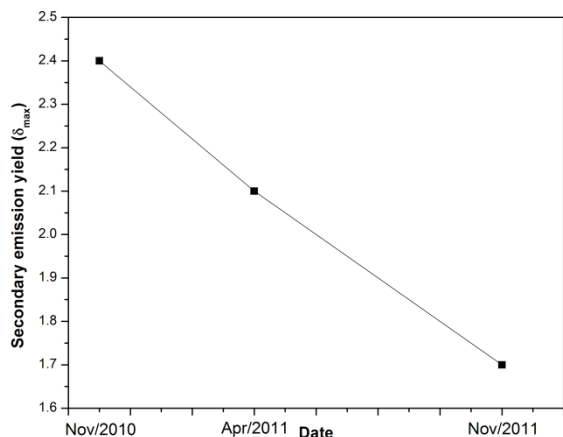


Figure 4: Evolution of δ_{max} for the LHC arc chamber during the 2011 LHC run as inferred from benchmarking heat-load simulations and measurements at 25-ns and 50-ns bunch spacing, assuming a low-energy electron reflectivity $R = 0.5$.

CONCLUSIONS

For the nominal LHC operation scheme with 25-ns bunch spacing at top energy, the maximum secondary-emission yield should be below 1.4 in order to reach the nominal bunch intensity with acceptable heat load.

For the current operational mode of the LHC the calculations at 50-ns bunch spacing show acceptable heat load values for all combinations of δ_{max} and R .

The simulated heat-load values can be compared with measured heat-load data for 50-ns and 25-ns bunch spacing in order to estimate the actual surface parameters (especially δ_{max}) for the LHC and their evolution in time. In this way the progress of surface conditioning during the 2011 LHC run has been deduced for the LHC arc chambers, with the result shown in Fig. 4.

ACKNOWLEDGMENTS

The work presented here has been cofunded by the Mexican National Council on Science and Technology (CONACYT) and by the European Commission under the FP7 Research Infrastructures project EuCARD, Grant Agreement No. 227579 (EuCARD-AccNet).

The authors would like to thank to Chandra Bhat, Gianluigi Arduini, Octavio Dominguez and Silvano Roubatel for their help and support of this work.

REFERENCES

- [1] LHC Design Report No. CERN-2004-003-V-1, 2004, Vol. 1, Chapter 2.
- [2] I. Collins (private communication), 1999.
- [3] V. Baglin, I. R. Collins and O. Groebner, in Proceedings of the 6th European Particle Accelerator Conference, Stockholm 1998 (Ref. [2]).
- [4] N. Hilleret, in CERN Accelerator Performance Committee Meeting of 1 August 2003.
- [5] D. Schulte and F. Zimmermann, in Proceedings of ELOUD'04, Napa, California, 2004, edited by M. Furman, S. Henderson, and F. Zimmermann (CERN Report No. CERN-2005-001, 2005).
- [6] M. A. Furman and V. H. Chaplin, Phys. Rev. ST Accel. Beams **9**, 034403 (2006).
- [7] LHC filling schemes website; http://lpc.web.cern.ch/lpc/documents/FillPatterns/50ns_1380b_1331_0_1320_144bpi12inj.txt
- [8] R. Bailey and P. Collier, LHC Project Note No. LHC-Project Note 323_Revised (2003).
- [9] G. Iadarola, at the LHC E-cloud Meeting on 28 November 2011; https://project-ecloud-meetings.web.cern.ch/project-ecloud-meetings/2011/28.11.2011/PyELOUD_ELOUDmeeting2811.pptx